Paramagnetic neutron scattering from the Heisenberg ferromagnet EuO

P. Böni and G. Shirane
Brookhaven National Laboratory, Upton, New York 11973
(Received 1 August 1985; revised manuscript received 29 October 1985)

Paramagnetic neutron scattering from the insulating Heisenberg ferromagnet EuO has been studied through the entire Brillouin zone. The measured linewidth Γ of the quasielastic scattering at T_c follows the predictions of dynamic scaling $\Gamma = Aq^{2.5}$ up to momentum transfers $q = 0.4$ Å^{-1}. The new results disagree with an early work by Passell *et al.*, where a smaller exponent and smaller linewidths have been reported, but agree perfectly with recent spin-echo measurements performed by Mezei at very small q. The $q^{2.5}$ dependence of Γ is now established over nearly four decades in energy. At large momentum transfers the energy distribution evolves into a three-peaked structure with much more spectral weight near $E = 0$, in disagreement with the two-peaked structure reported by Mook. The cross sections near the zone boundary are in quantitative agreement with recent calculations by Young and Shastry. We conjecture that peaks at finite energy occur in EuO and EuS because of the short-ranged exchange interactions.

I. INTRODUCTION

The magnetic properties of the isotropic Heisenberg ferromagnets EuO and EuS have been studied extensively in the past by several[1] experimental and theoretical methods.[2,3] The reason is that these systems are believed to be some of the most ideal realizations of the isotropic Heisenberg model. The theory of these systems is in a relatively advanced state (as compared to itinerant systems) and many predictions have been confirmed by experiment as demonstrated for example in a series of papers[4] by Passell, Dietrich, and Als-Nielsen.

Recently, more attention has been given to these systems for several reasons. During the last few years paramagnetic scattering from the itinerant systems Fe and Ni has been investigated in detail[5–11] by using polarized neutrons. The interpretation of the experimental results is controversial and no consensus has been reached until now as to whether the paramagnetic scattering at large momentum transfer q is purely diffusive or not. EuO and EuS, on the other hand, are the only known isotropic cubic ferromagnets where peaks at finite energy have been reported[12,13] unambiguously near the zone boundary indicating propagating modes. The measured energy distributions are at least in qualitative agreement with recent theories developed by Young and Shastry[2] and Lindgard.[3] It is therefore important to perform more detailed measurements at large q in the paramagnetic phase of EuO to test these theories in a more quantitative way and to answer some questions regarding the conditions under which propagating modes exist above T_c.

The q dependence of the linewidth Γ in EuO at the Curie temperature T_c is still contradictory. Recent spin-echo measurements performed by Mezei on EuO at small momentum transfer[14] verify the dynamical scaling prediction[15] at T_c

$$\Gamma = Af(\kappa_1/q)q^{\delta}, \tag{1}$$

where $f(\kappa_1/q) = 1$ and $\delta = 2.5$. The measured constant A and the exponent δ are, however, in disagreement with the early neutron scattering studies of Passell *et al.*[4] and new experiments are needed to resolve the discrepancies.

We present in this paper, new inelastic neutron scattering experiments performed on a powder sample of ^{153}EuO. Powder averaging should be no problem because of the very high isotropy[16] of EuO. The new data cover the entire Brillouin zone and show how the scattering evolves from a single peak at $E = 0$ into a more complicated structure than that reported originally by Mook[12] and how the energy width of the scattering saturates near the zone boundary. The overall behavior of the scattering at small q is well described by a double-Lorentzian scattering function as in Ni and Fe. Finally we will discuss the implications of our new results for other cubic ferromagnets.

II. EXPERIMENTAL

The measurements were performed on the same polycrystalline sample of ^{153}EuO used in the previous studies by Passell *et al.*[4] and Mezei.[14] The sample weighed 0.745 g, was 24.1 mm high, 11.5 mm wide, and 0.50 mm thick. EuO crystallizes in the NaCl structure with a lattice constant $a = 5.12$ Å^{-1} and a nearest inverse plane distance $d^*_{111} = 2.12$ Å^{-1}. The sample was mounted in a He-flow Dewar positioned on different triple axis spectrometers at the Brookhaven High Flux Beam Reactor. The temperature was measured by means of a platinum resistor with an accuracy of ± 0.02 K. We have determined the Curie temperature by measuring the temperature dependence of the critical scattering and obtained $T_c = 69.25 \pm 0.05$ K in good agreement with values reported in the literature.

All the data were collected in the forward direction keeping fixed the final neutron energy E_f. Pyrolytic graphite crystals set for the (002) reflection were used as monochromator and analyzer for most of the experiments. The cold source with a double monochromator system

provided the neutrons for the measurements at small momentum transfer $q \leq 0.2$ Å^{-1}. The final energy E_f was kept fixed at 2.5 or 4 meV. Higher-order neutrons were removed by a cooled Be filter placed before the sample. The measurements for $q \geq 0.3$ Å^{-1} were conducted on thermal neutron sources with $E_f = 14$ meV (Ge monochromator, no filter) or $E_f = 14.7$ meV with a pyrolytic graphite filter mounted after the sample to remove higher-order contamination. The collimations are defined in the figure headings. All data measured with $E_f = 14.7$ meV have been corrected because higher-order neutrons are also reflected by the pyrolytic graphite monochromator and are therefore detected by the monitor counter. The correction factor decreases monotonically from 1 at $E_i = 14.7$ meV to 0.79 at $E_i = 19.7$ meV (corresponding to 5-meV energy transfer) and has been measured accurately.[17]

We have put the energy-integrated paramagnetic scattering $S(q)$ onto an absolute scale by comparing the integrated intensity of magnons below T_c (counts/min) with the calculated cross section (barns/sr) following the procedure of Wicksted *et al.*[7] The data can then be converted into units of the Bohr magneton squared (μ_B^2) using

$$M^2(Q) = \frac{S(q)(\text{in barns/sr})}{0.0485 f^2(Q) e^{-2W}} , \tag{2}$$

where $f(Q)$ is the form factor and e^{-2W} is the Debye-Waller factor. This conversion is valid only if the energy scale of the scattering is smaller than $k_B T$. For EuO the conversion is valid.

III. SPECTRAL WEIGHT FUNCTIONS

Before presenting our new data we would like to introduce some spectral weight functions $F(q,\omega)$, which appear frequently in magnetic cross sections for $T \geq T_c$

$$\frac{d^2\sigma}{d\Omega\, d\omega} = \gamma_0^2 \frac{k_f}{k_i} \left| \frac{1}{2} g f(Q) \right|^2 \times e^{-2W} 2 k_B T \chi(q) F(q,\omega) \frac{\hbar\omega/k_B T}{1 - e^{-\hbar\omega/k_B T}} , \tag{3}$$

where $\gamma_0^2 = 0.291$ barns/sr, k_f and k_i are the wave vectors of the final and incident neutrons, and g is the gyromagnetic ratio. The wavelength-dependent susceptibility $\chi(q)$ is usually expanded to the second order in q as

$$\chi(q) = \chi(0) \frac{\kappa_1^2}{\kappa_1^2 + q^2} , \tag{4}$$

where $\kappa_1 = \kappa_0 [(T - T_c)/T_c]^{\nu}$ is the inverse correlation length and $\chi(0)$ is the bulk (dc) susceptibility.

The diffusive scattering is usually well approximated by a simple Lorentzian ($\epsilon = 1$)

$$F_L(q,\omega) = \frac{1}{\pi} \left[\frac{\Gamma}{\Gamma^2 + \omega^2} \right]^{\epsilon(\omega)} . \tag{5}$$

To parametrize the expected[18] and measured[4,7] deviations of the spectrum from a pure Lorentzian we have introduced an additional parameter $\epsilon(\omega)$ defined by $\epsilon = 1$ for $|\omega| \leq \Gamma$ and $\epsilon = 1 + \alpha(|\omega| - \Gamma)/\Gamma$ for $|\omega| > \Gamma$, where α is a constant. This modification of a Lorentzian by the additional α is, of course, an empirical approach to parametrize the scattering function. A recent theoretical paper by Folk and Iro[19] gives some justification for this as we shall discuss in a future publication.

The damped harmonic oscillator function

$$F_H(q,\omega) = \frac{1}{\pi} \frac{\gamma \omega_0^2}{(\omega^2 - \omega_0^2)^2 + \gamma^2 \omega^2} \tag{6}$$

is useful to parametrize heavily damped excitations and has been used by Mook[12] to analyze the EuO data. $F_H(q,\omega)$ is equivalent to Lorentzian peaks at $\pm\omega_0$ with $\Gamma = \gamma/2$ if $\gamma \ll \omega_0$. Another useful form is the three-pole approximation[2,13,20]

$$F_S(q,\omega) = \frac{1}{\pi} \frac{\tau \delta_1 \delta_2}{\omega^2 \tau^2 (\omega^2 - \delta_1 - \delta_2)^2 + (\omega^2 - \delta_1)^2} , \tag{7}$$

with $\tau = (\pi\delta_2/2)^{-1/2}$ and the frequency moments $\delta_1 = \langle \omega^2 \rangle_q$ and $\delta_2 = \langle (\omega^2 - \langle \omega^2 \rangle_q)^2 \rangle_q$. $F_S(q,\omega)$ exhibits one peak if $\delta_2 \geq 2\delta_1$ and three peaks if $\delta_2 < 2\delta_1$. To understand the structure of $F_S(q,\omega)$ better we rewrite it in the more transparent form

$$F_S(q,\omega) = \frac{1}{\pi} \frac{\gamma \omega_0^2}{(\omega^2 - \omega_0^2)^2 + \gamma^2 \omega^2 \left[\dfrac{\omega^2 - \omega_0^2 - \frac{\pi}{2}\gamma^2}{\frac{\pi}{2}\gamma^2} \right]^2} \tag{8}$$

with $\gamma = (2\delta_2/\pi)^{1/2}$ and $\omega_0^2 = \delta_1$. Equation (8) resembles a damped harmonic oscillator; for $\omega^2 \simeq \omega_0^2$ they are identical. The half-width at half maximum (HWHM) Γ of $F_S(q,\omega)$ can be obtained by solving a linear equation in Γ^2 of degree three with coefficients depending on δ_1 and δ_2. Γ is uniquely defined as long as one real root exists only. An alternative possibility to characterize the width of the energy distribution is the half-area width $\omega_{1/2}$. It is defined by the relation[20]

$$\int_{-\omega_{1/2}}^{\omega_{1/2}} F(q,\omega)\, d\omega = \tfrac{1}{2} \int_{-\infty}^{\infty} F(q,\omega)\, d\omega .$$

$\omega_{1/2}$ is uniquely defined for each pair (δ_1,δ_2) and is equal to Γ, if $F(q,\omega)$ is a Lorentzian. Below T_c, $\omega_{1/2}$ is defined too and equal to the spin-wave energy.

IV. PARAMAGNETIC SCATTERING ABOVE T_c

Most of the measurements were performed in the constant-q mode of operation. We have determined background contributions and the absolute cross-section scale by conducting constant-q scans below T_c where the sample is in its ferromagnetic phase. Typical scans are shown in the upper parts of Figs. 1 and 2 for $q = 0.12$ Å^{-1} (cold source) and for $q = 0.30$ Å^{-1}. The solid lines through the data points have been obtained by a least-squares fitting procedure assuming a cross section for the scattering (convoluted with the resolution function), which includes a

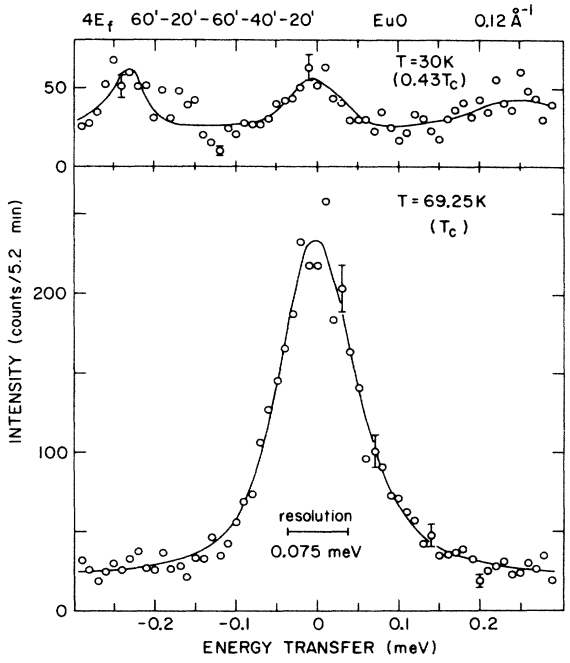

FIG. 1. Constant-q scans performed at the cold source. The solid lines are fits to the data as explained in the text.

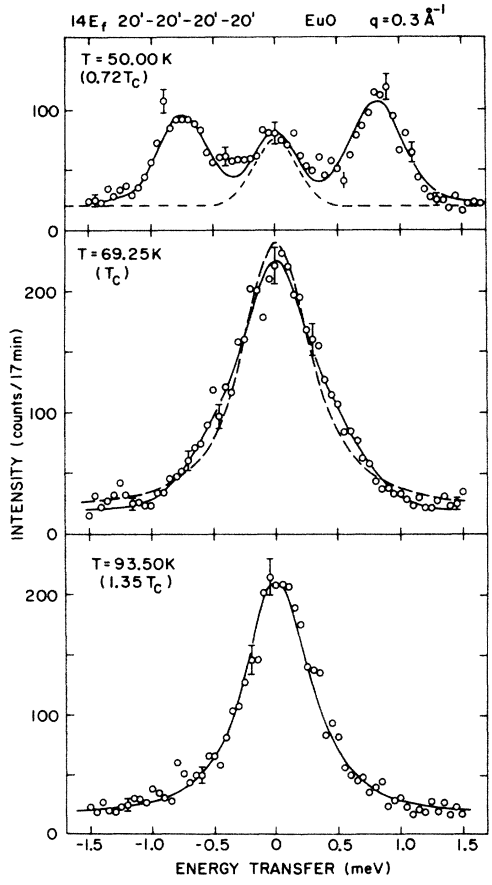

FIG. 2. Constant-q scans obtained for intermediate momentum transfer. The solid lines are fits to the data. The scan at $T=T_c$ deviates significantly from a pure Lorentzian (dashed line).

Lorentzian for the magnons, a constant (room) background and an elastic peak which is mostly due to incoherent scattering. The fits indicate that the nonmagnetic scattering can be separated out reliably.

The solid lines through the (raw) data at and above T_c represent fits to Lorentzians in q and ω given by Eqs. (4) and (5) including the fixed background contributions. At $q=0.12$ Å^{-1}, the exponent ϵ has been kept fixed at 1, whereas at $q=0.3$ Å^{-1}, the modified form with floating

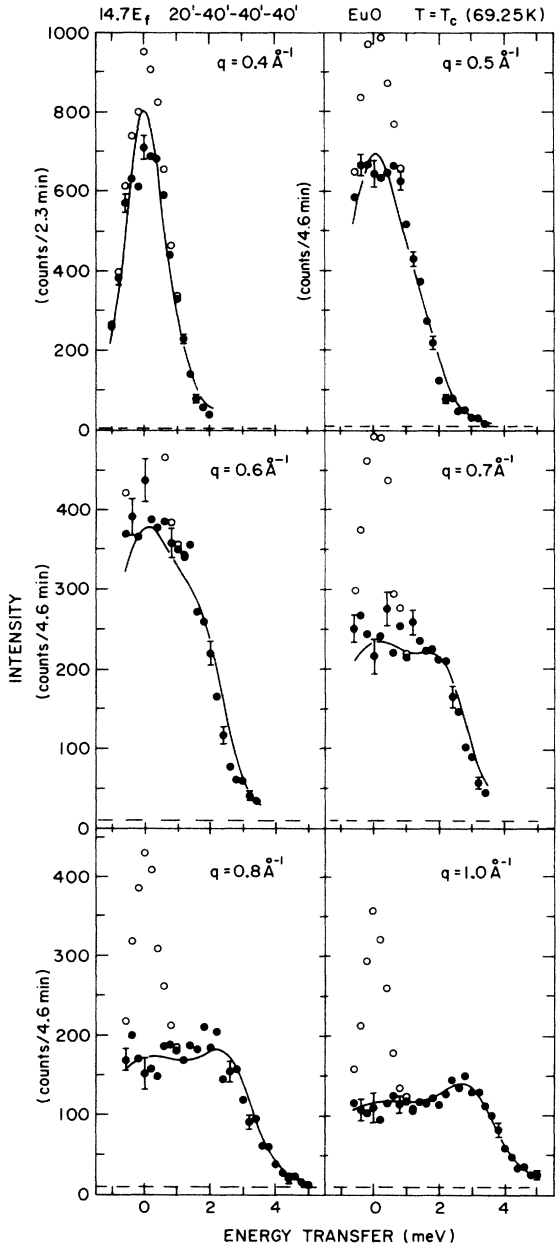

FIG. 3. The collection of constant-q scans at $T=T_c$ demonstrates clearly the appearance of peaks at finite energy for $q>0.5$ Å^{-1}, in agreement with the theoretical calculations from Ref. 2, indicated by solid lines. The solid circles have been obtained after subtracting a nonmagnetic elastic peak (see Fig. 5) from the raw data (circles). The dashed curve indicates the constant room background.

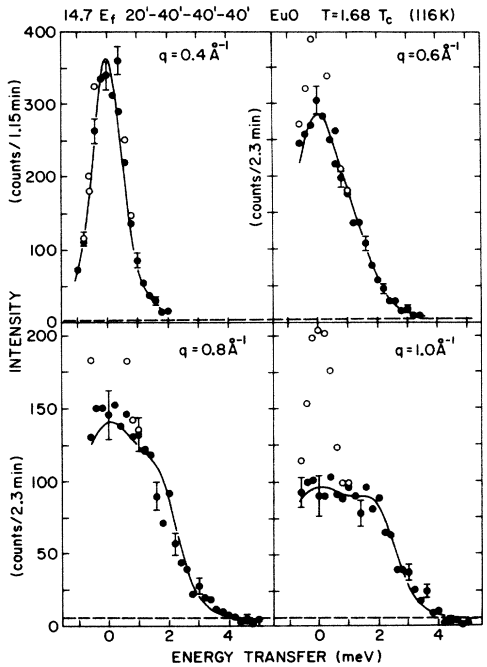

FIG. 4. Similar data as in Fig. 3, obtained at $T=1.68T_c$. Shoulders develop above $q=0.6$ Å^{-1}. The symbols have the same meaning as in Fig. 3.

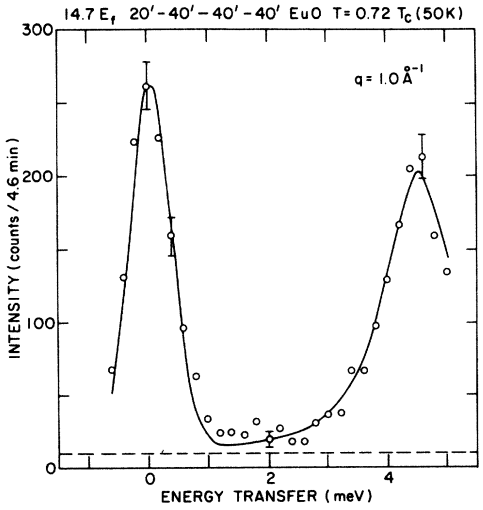

FIG. 5. Typical constant-q scan performed below T_c to determine the background contributions. The fitted (resolution convoluted) cross section consists of a δ function for the elastic peak and a Lorentzian for the spin wave at 4.5 meV. The dashed curve indicates the constant room background.

α has been used to take properly the clearly visible deviations of the data from a pure Lorentzian into account. The fits yielded $\alpha=1.6\pm0.4$ at T_c and $\alpha=0.22\pm0.08$ at $1.35T_c$. Equally good fits have been obtained when we used the three-pole approximation, yielding the same linewidths, i.e., 0.46 ± 0.04 meV at $T=T_c$, whereas pure Lorentzians (broken line in Fig. 2) never fitted the data well and yielded significantly smaller linewidths, i.e., 0.29 ± 0.02 meV at $T=T_c$. The strong temperature dependence of the peak profile is clearly visible in Fig. 2. At higher temperature it resembles more a Lorentzian than at T_c, as expected.[18,21] The narrowing of the peaks is in quantitative agreement with the predictions of Résibois and Piette[22] and the previous study by Passell[4] *et al.*

The measurements depicted in Figs. 3 and 4 demonstrate how the peak profile changes dramatically with increasing q. The filled circles represent the data obtained after subtracting a nonmagnetic elastic peak at $E=0$. Its magnitude has been determined from constant-q scans at 50 K. One typical scan conducted near the zone boundary is given in Fig. 5 and the solid line is a fit to the data as described above. The broken lines in Figs. 3 and 4 indicate the small constant room background. The solid lines are actually model calculations, discussed in Sec. V, and are in good agreement with the observations. We have determined the HWHM and the half-area width $\omega_{1/2}$ from δ_1 and δ_2 by fitting the data in Figs. 3 and 4 to Eq. (3), assuming again a Lorentzian behavior for $\chi(q)$ [see Eq. (4)] and a three pole approximation for $F(q,\omega)$. The fitted parameters δ_1 and δ_2 are given in Table I, together with the corresponding linewidths and $\omega_{1/2}$. It is evident from Table I that $\omega_{1/2}$ at $1.68T_c$ is about 60% of $\omega_{1/2}$ obtained at T_c for fixed q. This decrease agrees astonishingly well (even near the zone boundary) with the predictions

TABLE I. Comparison of predicted (Refs. 2 and 28) and fitted parameters δ_1 and δ_2 [see Eq. (7)] in meV^2. Also given are the linewidth (HWHM) and the half-area width ($\omega_{1/2}$) in meV as calculated from δ_1 and δ_2.

Units of		Theory		Experiment			
T (T_c)	q (Å^{-1})	δ_1	δ_2	δ_1	δ_2	HWHM	$\omega_{1/2}$
1	0.4	0.559	2.76	0.42±0.02	1.1±0.1	0.84	0.45
1	0.5	1.19	3.66	0.96±0.04	2.6±0.2	1.22	0.67
1	0.6	2.09	4.84	1.70±0.05	4.0±0.2	1.85	0.95
1	0.7	3.16	6.18	2.65±0.07	5.3±0.3	2.45	1.26
1	0.8	4.23	7.50	3.81±0.10	7.1±0.4	2.98	1.55
1	1.0	5.65	9.19	5.70±0.07	8.9±0.4	3.70	2.01
1.68	0.4	0.394	2.81	0.34±0.03	2.0±0.4	0.34	0.29
1.68	0.6	1.10	3.47	1.09±0.04	3.8±0.3	0.92	0.65
1.68	0.8	1.99	4.21	1.89±0.08	5.3±0.5	1.63	0.93
1.68	1.0	2.56	4.70	2.50±0.15	4.7±0.6	2.41	1.25

of Résibois and Piette,[22] who derived the dynamical scaling function $f(\kappa_1/q)$ in the limit $q \simeq 0$ and $T \simeq T_c$. Note, that the modified Lorentzian, Eq. (5), is capable of describing the data up to 0.5 Å^{-1} only.

In Fig. 6 we have plotted the HWHM versus q on a log-log scale as obtained in this study and as measured by Mezei.[14] The linewidth follows the dynamical scaling prediction $\Gamma \alpha q^{2.5}$ over nearly 4 decades in energy. Above $q > 0.4$ Å^{-1} the linewidth starts to saturate. The solid line is a fit with $A = 8.3 \pm 0.7$ meV Å$^{2.5}$ and $\delta = 2.50 \pm 0.07$. The expected deviations from dynamical scaling at higher q are more clearly visible in a linear Γ versus q representation (Fig. 7), where we compare the HWHM (triangles) with $\omega_{1/2}$ (circles). Up to $q \simeq 0.2$ Å^{-1} both measures agree with each other, indicating that the spectral weight function closely resembles a Lorentzian where $\omega_{1/2} \equiv \Gamma$. Above $q \simeq 0.3$ Å^{-1} the two measures deviate from each other more and more with increasing q, in agreement with the experimental observation that the shape of $F(q,\omega)$ changes with q (see Figs. 2–4). We conclude that a pure Lorentzian is not the appropriate form to fit the data at $q > 0.2$ Å^{-1}. This may be one of the reasons why a smaller exponent ($\delta = 2.29$) and smaller linewidths have been obtained[4] in a previous study of EuO (see Fig. 6).

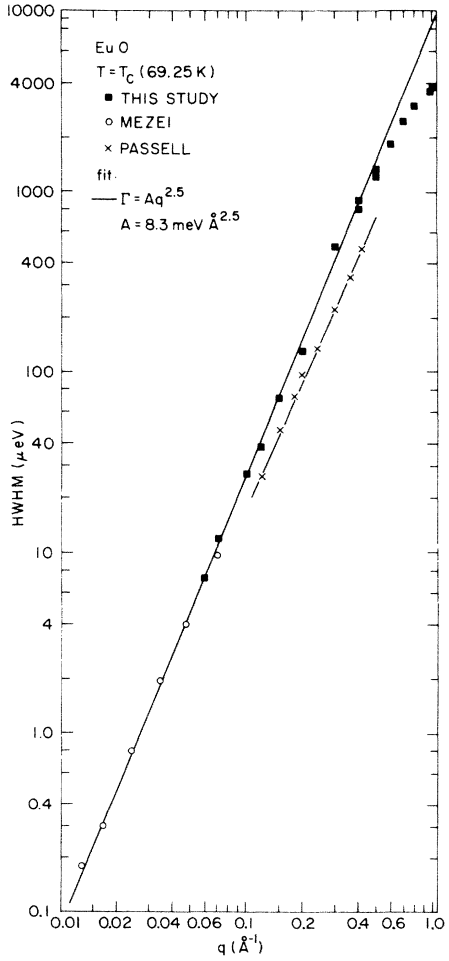

FIG. 6. Linewidth versus q in a log-log representation. The data from Ref. 14 and our data follow perfectly the dynamical scaling prediction $\Gamma \alpha q^{2.5}$ over 4 decades in energy.

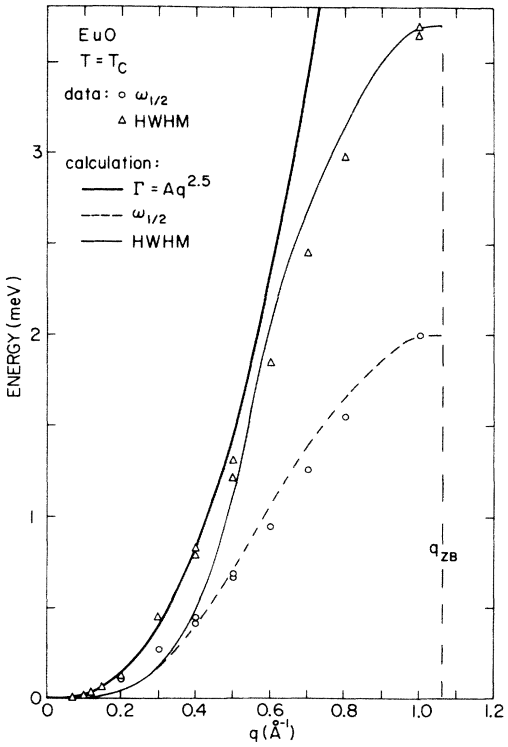

FIG. 7. The linewidth (HWHM) and the half-area width $\omega_{1/2}$ plotted versus q. In the small-q region the data follow the dynamical scaling predictions. The measurements near the zone boundary are in good agreement with the theoretical predictions from Ref. 2.

Finally we would like to present some energy-integrated data $M^2(Q)$, which has been put into an absolute scale as described in Sec. II. The Debye-Waller factor is always

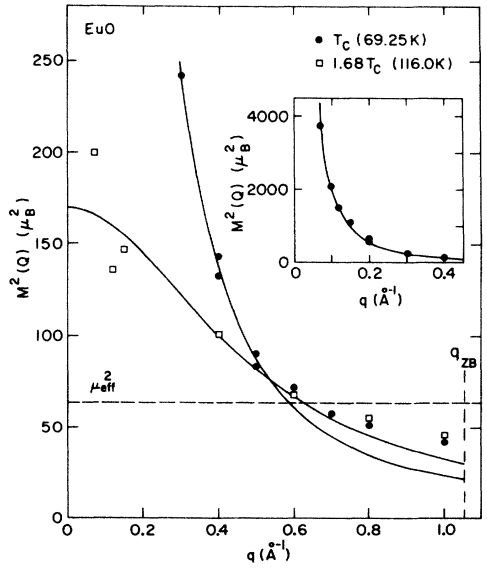

FIG. 8. Integrated intensity $M^2(Q)$ vs q. Near the zone boundary (ZB) the measured intensity is higher than predicted by a Lorentzian (solid lines). The dashed line indicates $\mu_{\text{eff}}^2 = 63\mu_B^2$.

TABLE II. Cubic ferromagnets. A^* and κ_0^* are expressed in units of reduced wave number ζ of the inverse plane distance d^*. Note a narrow range of κ_0^*, in contrast to a very large variation of A^*. d^* corresponds to (110) for Fe and (111) for other ferromagnets. n is the number of important exchange constants J_n. ($\Gamma = Aq^{2.5}$ at T_c, $A^* = A(d^*)^{2.5}$, $\kappa_1^* = \kappa_0^*[(T-T_c)/T_c]^{0.7}$.)

	Ni	Fe	Pd_2MnSn	EuO
T_c (K)	627	1043	190	69.2
A (meV $A^{2.5}$)	350	140	60	8.3
A^* (meV)	5900	2400	230	53
A^*/T_c (meV K)$^{-1}$	9.4	2.3	1.2	0.77
κ_0 (Å^{-1})	0.62	1.05	0.37	0.64
κ_0^* (units of ζ)	0.20	0.34	0.22	0.30
lattice constant a (Å)	3.5	2.9	6.4	5.1
d^* (Å^{-1})	3.1	3.1	1.7	2.1
n			>6	≈ 2

larger than 0.98 during our experiments and has been set equal to 1 for convenience. The solid lines through the data points in Fig. 8 represent Lorentzians

$$M^2(Q) = M^2(0)\frac{\kappa_1^2}{\kappa_1^2 + q^2}, \tag{9}$$

where κ_1 has been taken from Ref. 4 (see Table II) and $M^2(0)$ has been fixed so that $M^2(Q)$ reproduces the data at $q = 0.4$ Å^{-1}. For $T = 116$ K we obtain $M^2(0) = 170\mu_B^2$ in close agreement with $180\mu_B^2$ as obtained from static susceptibility measurements[23] by Menyuk *et al.* The scatter of the small-q data at 116 K is large because of the small scattering intensity at this high temperature as compared to the T_c data (see inset). The q^2 expansion (Eq. 9) for $M^2(Q)$ is not expected to be valid at larger q and our measurements indeed demonstrate that the measured intensity near the zone boundary is larger than expected for pure Lorentzian behavior. A similar behavior has been observed in the Heisenberg system[24] Pd_2MnSn, in contrast to that in the itinerant systems Ni (Ref. 5) and Fe (Refs. 5, 7, and 8), where the measured intensity $M^2(Q)$ is smaller at large q. The larger intensity for Heisenberg systems is expected because the moment $M^2(Q)$, integrated over the whole Brillouin zone, must be conserved. Therefore the zone-boundary intensity at $1.68T_c$ is larger than at T_c (see Fig. 8) to compensate for the smaller moment $M^2(Q)$ at small q. If we only integrate the areas below the Lorentzians in Fig. 8, we obtain $56\mu_B^2$ for $T = T_c$ and $51\mu_B^2$ for $1.68T_c$, whereas an integration of the measured intensity yields $69\mu_B^2$ and $63\mu_B^2$, respectively, in good agreement with the high-temperature limit $\mu_{\text{eff}}^2 = 63\mu_B^2$.

V. DISCUSSION

The qualitative behavior of our EuO data confirms previous measurements by Mook performed on a single crystal. There is, however, one very important difference between the two studies. Our constant-q profiles, measured near the zone boundary, reveal much more intensity around $E = 0$ and cannot be adequately analyzed in terms of a damped harmonic oscillator function as demonstrated in Fig. 9. The dashed line has been calculated using Eq. 6 (with the parameters $\omega_0 = 2.98$ meV and $\gamma = 1.74$ meV from Ref. 12) convoluted with our resolution function. The additional intensity around $E = 0$ cannot be explained by an improper subtraction of the elastic peak: it would produce either a peak or a dip in the data at $E = 0$ with a resolution width (HWHM) of 0.4 meV. This is not observed. Scattering by magnetic disorder may occur around $E = 0$ if part of the magnetic Eu^{2+} ions had been converted into nonmagnetic Eu^{3+} by aging. Again, the (elastic) peak would be resolution limited and should be seen. In addition, if there was no additional intensity at $E = 0$ the moment $M^2(Q)$, integrated over the Brillouin zone, would be significantly smaller than $\mu_{\text{eff}}^2 = 63\mu_B^2$ and be in disagreement with the underlying assumptions for a Heisenberg model. We conclude that the broad peak at $E = 0$ is real and persists up to the zone boundary.

At first glance one might interpret the central peak as a diffusive peak, corresponding to a quasielastic longitudinal component below T_c, as predicted by Mazenko,[25] and the peak at finite energy as a not fully renormalized spin wave (transverse component). This interpretation, however, is not unique. At this stage we cannot rule out the possibility that the longitudinal component already exhibits three peaks just below T_c, as predicted by Vaks *et al.*[26] Villain,[27] on the other hand, suggested two inelastic peaks at the spin-wave frequencies. This prediction would ex-

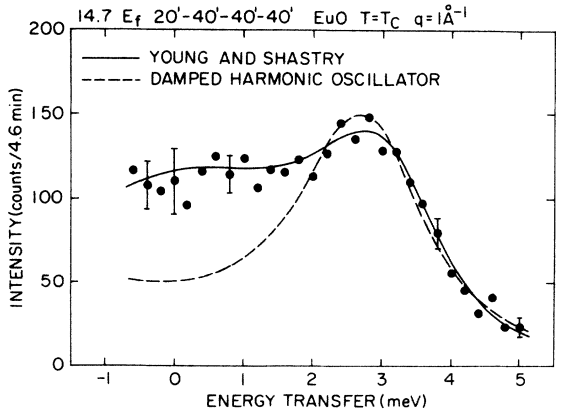

FIG. 9. The data from Ref. 12 (dashed line) measured at the [111] zone boundary is compared with our data at $q = 1.0$ Å^{-1}. Our data is well characterized by the three pole approximation from Ref. 2.

plain why no central component has been observed[4] below T_c at small q but would not explain our observed peak at $E=0$ near the zone boundary. The above-mentioned theories[25–27] have been deduced for small q only and are not necessarily valid in the q range investigated in this study. Further experiments just below T_c are planned in the near future to elucidate the predicted scenarios further and to check their universality.

There exist two microscopic approaches which predict the lineshapes in the paramagnetic phase of EuO and EuS. Lindgard has used a correlation theory[3] for one dynamical variable and obtained to lowest order a damped harmonic oscillator function, which represented the data from Ref. 12 well. At the same time Young and Shastry have succeeded in calculating the frequency moments of the spectral weight function in terms of static correlation functions using a three pole approximation.[2] Although both theories predict the occurrence of a "spin-wave" peak at large q correctly, only the three pole approximation $F_S(q,\omega)$ [Eq. (7)] predicts a central peak and has therefore been utilized by us to analyze our data.

Before comparing our data with theory it is important to discuss possible complications introduced by powder averaging of our sample in an experiment. In Fig. 10 we have plotted the predicted peak shapes[28] $F_S(q,\omega)$ for $q=1.06$ Å^{-1} (the zone boundary distance in the [111] direction) for the [111], [110], and [100] directions. The scattering is very isotropic, in fact, the peak positions do not deviate by more than half the resolution width (0.4 meV) from each other. In particular the profile of the central peak is not affected by powder averaging.

To facilitate the comparison with experiment we therefore neglected the powder broadening of the data and have calculated peak profiles for the [111] direction only. The solid lines in Figs. 3, 4, and 9 have been obtained by convoluting the cross section with the resolution function, using values for δ_1 and δ_2 provided by Shastry and Chaudhury.[28] The normalization constant, say N, has been fixed for each scan in such a way that χ^2 was minimized. N was constant at small q and independent of temperature, but increased by nearly a factor of 2 between $q=0.5$ and $q=1$ Å^{-1} because of the deviations of $M^2(Q)$ from a pure Lorentzian (see Fig. 8). The agreement between experiment and theory is excellent (see also Table I) and confirms that the scattering mechanism is well understood, at least at large momentum transfers. At small q, however, the predicted linewidths are too small (Fig. 7) and the dynamic scaling prediction $\delta=2.5$ is violated. Similar discrepancies have also been observed in Fe (Ref. 7) and they occur because the higher-frequency moments, which are important at small q, are neglected in the three pole approximation. In the small-q region it is more appropriate to compare the linewidth measurements with the dynamic scaling approach performed by Riedel[29] or Hubbard[21] who predict[4] $A=6.4$ meV Å$^{2.5}$ and $A=7$ meV Å$^{2.5}$, respectively. These values are in good agreement with the experimental value $A=8.3\pm0.7$ meV Å$^{2.5}$. Our experiments confirm the conclusion, reached in a previous study,[14] that no crossover to dipolar dynamics near $q_d=0.147$ Å^{-1} occurs. It is fair to say that the dynamical properties of EuO above T_c are well understood.

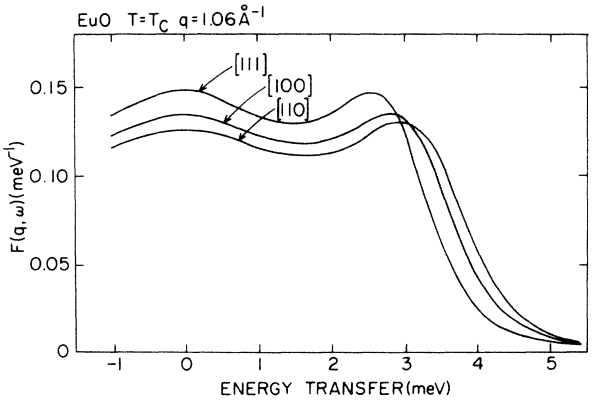

FIG. 10. Predicted line shapes at $q=1.06$ Å^{-1} for three principal directions, demonstrating the high isotropy of the scattering at the nearest zone boundary.

The paramagnetic scattering from EuO behaves similarly to that reported for other isotropic cubic ferromagnets like the localized metallic system[24] Pd_2MnSn and the itinerant systems[6–10] Fe and Ni. The scattering follows the predictions of a modified double-Lorentzian scattering function up to about halfway to the zone boundary. At larger q the width of the energy distribution saturates in a similar way as in the above systems. There are at least two obvious reasons for this. (1) The energies involved are not small compared with T, hence the system is no longer in the critical region, where dynamical scaling is valid. (2) The energy scale in a Heisenberg system is limited and of the order of k_BT_c.

Finally we would like to address the question of why peaks at finite energy definitely occur at large q in EuO and EuS, but not in Pd_2MnSn, Fe, and Ni. In Table II we have listed some relevant parameters for these systems. The inverse correlation lengths, characterized by κ_0 and κ_0^*, are obviously very similar for all systems and are therefore not related to the appearance of peaks at finite energy even if $q\gg\kappa_1$. The constant A, or in reduced ζ units A^*, and T_c are very different, however, if A^* is properly scaled by T_c we find that $A^*/T_c\simeq1$ for the Heisenberg systems whereas $A^*/T_c\gg1$ for Fe and Ni. Note that the ratio A^*/T_c may be used as a measure for the itinerancy of the electrons.[24] Although the ratio is very similar in Pd_2MnSn and EuO, no peak at finite energy has been observed in Pd_2MnSn. Therefore, A and T_c are also no signature for the appearance of peaks at finite energy, as hinted in a recent report by Lynn.[30] There is, however, one important difference between the two localized systems: To reproduce adequately the spin-wave dispersion curves below T_c, more than six exchange parameters have to be included for Pd_2MnSn,[31] whereas two are sufficient for EuO or EuS.[32] In other words the exchange interactions are longer ranged in Pd_2MnSn. The peaks at finite energy in EuO or EuS may be a remainder of a heavily damped zone-boundary spin wave mediated by the exchange between nearest and next-nearest neighbors. The spins in Pd_2MnSn, on the other hand, are ex-

posed to a more complicated and longer-ranged field generated by the thermal motion of the spins, which smear out or dampen possible excitations at finite energy, yielding a single-peaked structure even at the zone boundary. If the above explanation for the appearance of peaks is correct, we do not expect to find any excitations in Ni and Fe above T_c because of the itinerant nature of the electrons, in agreement with all our recent experiments on Fe and Ni.[6–10]

ACKNOWLEDGMENTS

It is a pleasure to acknowledge very stimulating discussions with R. Chaudhury, H. G. Bohn, Y. Endoh, M. Koghi, F. Mezei, L. Passell, G. F. Reiter, S. M. Shapiro, B. S. Shastry, Y. J. Uemura, and J. P. Wicksted. The work at Brookhaven National Laboratory was supported by the Division of Materials Sciences, U. S. Department of Energy under Contract No. DE-AC02-76CH00016.

[1]For a review, see P. Wachter, in *Handbook on the Physics and Chemistry of Rare Earths,* edited by K. A. Gschneidner and L. Eyring (North-Holland, Amsterdam, 1979), Vol. 2, Chap. 19.

[2]A. P. Young and B. S. Shastry, J. Phys. C **15**, 4547 (1982).

[3]Per-Anker Lindgard, J. Appl. Phys. **53**, 1861 (1982); Phys. Rev. B **27**, 2980 (1983).

[4]L. Passell, O. W. Dietrich, and J. Als-Nielsen, Phys. Rev. B **14**, 4897 (1976); **14**, 4908 (1976); **14**, 4923 (1976).

[5]P. J. Brown, H. Capellmann, J. Déportes, D. Givord, and K. R. A. Ziebeck, J. Magn. Magn. Mater. **31-34**, 295 (1983).

[6]O. Steinsvoll, C. F. Majkrzak, G. Shirane, and J. P. Wicksted, Phys. Rev. Lett. **51**, 300 (1983); Phys. Rev. B **30**, 2377 (1984).

[7]J. P. Wicksted, P. Böni, and G. Shirane, Phys. Rev. B **30**, 3655 (1984).

[8]G. Shirane, P. Böni, and J. P. Wicksted, Phys. Rev. B **33**, 1881 (1986).

[9]P. Böni and G. Shirane, J. Appl. Phys. **57**, 3012 (1985).

[10]J. L. Martínez, P. Böni, and G. Shirane, Phys. Rev. B **32**, 7037 (1985).

[11]H. A. Mook and J. W. Lynn, J. Appl. Phys. **57**, 3006 (1985).

[12]H. A. Mook, Phys. Rev. Lett. **46**, 508 (1981).

[13]H. G. Bohn, A. Kollmar, and W. Zinn, Phys. Rev. B **30**, 6504 (1984).

[14]F. Mezei, J. Magn. Magn. Mater. **45**, 67 (1984).

[15]B. I. Halperin and P. C. Hohenberg, Phys. Rev. **177**, 952 (1969).

[16]See spin-wave dispersion curves, Fig. 2 from Ref. 1 (p. 4900).

[17]R. A. Cowley, G. Shirane, R. J. Birgeneau, and H. J. Guggenheim, Phys. Rev. B **15**, 4292 (1977).

[18]W. Marshall and S. W. Lovesey, *Theory of Thermal Neutron Scattering* (Oxford University Press, London, 1971).

[19]R. Folk and H. Iro, Phys. Rev. B **32**, 1880 (1985).

[20]S. W. Lovesey and R. A. Meserve, J. Phys. C **6**, 79 (1973).

[21]J. Hubbard, J. Phys. C **4**, 53 (1971).

[22]R. Résibois and C. Piette, Phys. Rev. Lett. **24**, 514 (1970).

[23]N. Menyuk, K. Dwight, and T. B. Reed, Phys. Rev. B **3**, 1689 (1971).

[24]G. Shirane, Y. J. Uemura, J. P. Wicksted, Y. Endoh, and Y. Ishikawa, Phys. Rev. B **31**, 1227 (1985).

[25]G. F. Mazenko, Phys. Rev. B **14**, 3933 (1976).

[26]V. G. Vaks, A. I. Larkin, and S. A. Pikin, Zh. Eksp. Teor. Fiz. **53**, 1089 (1967) [Sov. Phys.—JETP **26**, 647 (1968)].

[27]J. Villain, Solid State Commun. **8**, 31 (1970).

[28]We thank B. S. Shastry and R. Chaudhury for providing us with the values δ_1 and δ_2 for EuO.

[29]E. K. Riedel, J. Appl. Phys. **40**, 1197 (1971).

[30]J. W. Lynn, Phys. Rev. Lett. **52**, 775 (1984).

[31]Y. Noda and Y. Ishikawa, J. Phys. Soc. Jpn. **40**, 690 (1976).

[32]H. G. Bohn, W. Zinn, B. Dorner, and A. Kollmar, J. Appl. Phys. **52**, 2228 (1981).